Petroleum Science 19 (2022) 789–799

Contents lists available at ScienceDirect

Petroleum Science

journal homepage: www.keaipublishing.com/en/journals/petroleum-science

Rotational failure analysis of spherical-cylindrical shell pressure controllers related to gas hydrate drilling investigations

Cong Li [a, b], Jian-Liang Pei [a, *], Nian-Han Wu [a], Gui-Kang Liu [a], Wei Huang [a], Zhi-Xu Dai [c, d], Rui-Ze Wang [e], Zhao-Fan Chen [d], Wei-Cheng Long [e]

[a] MOE Key Laboratory of Deep Earth Science and Engineering, Sichuan University, College of Water Resource and Hydropower, Sichuan University, Chengdu, 610065, China
[b] Guangdong Provincial Key Laboratory of Deep Earth Sciences and Geothermal Energy Exploitation and Utilization, Institute of Deep Earth Sciences and Green Energy, College of Civil and Transportation Engineering, Shenzhen University, Shenzhen, 518060, China
[c] China Pingmei Shenma Energy and Chemical Industry Group Co., Ltd., Pingdingshan, 467000, China
[d] State Key Laboratory of Coking Coal Exploitation and Comprehensive Utilization, Pingdingshan, 467000, China
[e] Xi'an Research Institute, China Coal Technology and Engineering Group, Xi'an, 710077, China

ARTICLE INFO

Article history:
Received 1 July 2021
Accepted 21 December 2021
Available online 25 February 2022

Edited by Xiu-Qiu Peng

Keywords:
Exploration of oil and gas resources
Pressure coring controller
Sphere flapper valve
Failure modes
Stress deviation rate

ABSTRACT

In situ pressure-preserved coring (IPP-Coring) technology is considered one of the most efficient methods for assessing resources. However, seal failure caused by the rotation of pressure controllers greatly affects the success of pressure coring. In this paper, a novel spherical-cylindrical shell pressure controller was proposed. The finite element analysis model was used to analyze the stress distribution and deformation characteristics of the pressure controller at different rotation angles. The seal failure mechanism caused by the rotation of the pressure controller was discussed. The stress deviation rate was defined to quantitatively characterize the stress concentration. Based on the test equipment designed in this laboratory, the ultimate bearing strength of the pressure controller was tested. The results show that the rotation of the valve cover causes an increase in the deformation on its lower side. Furthermore, the specific sealing pressure in the weak zone is greatly reduced by a statistically significant amount, resulting in seal failure. When the valve cover rotates 5° around the major axis, the stress deviation rate is −92.6%. To prevent rotating failure of the pressure controller, it is necessary to control the rotation angle of the valve cover within 1° around the major axis. The results of this research can help engineers reduce failure-related accidents, provide countermeasures for pressure coring, and contribute to the exploration and evaluation of deep oil and gas resources.

1. Introduction

Natural gas hydrate is widely considered the most promising clean energy source for the future (Sloan, 2003; Pang et al., 2021). Countries worldwide are actively exploring the technology of natural gas-hydrates, which has greatly promoted the development of natural gas hydrates (Hu et al., 2021; Saberi et al., 2021; Gao et al., 2022). The potential impact of NGH development on the global carbon cycle (Dickens et al., 1997), sustainable environmental change (Archer, 2007), drilling hazards and future energy production (Boswell and Collett, 2011) are issues to be explored at the frontier of science (Singh et al., 1993). Scientific research mainly focuses on the following aspects:

- the development of exploration technology and equipment, including physical exploration technology and pressure coring technology, and the establishment of a scientific evaluation system (Jin et al., 2014; Gao et al., 2021; He et al., 2021; Huang et al., 2021; Kida et al., 2021),
- the study of the physical and mechanical properties of *in-situ* NGH and the development of economic and efficient mining methods (Konno et al., 2013; Jing et al., 2015; Aydin and Merey, 2021; Fu et al., 2021; Gao et al., 2021; Gao et al. 2021, 2021; Ruan et al., 2021), and

* Corresponding author.
E-mail address: peijl@scu.edu.cn (J.-L. Pei).

https://doi.org/10.1016/j.petsci.2022.02.005

Abbreviations

DAPC	Dynamic autoclave piston corer
DSDP	Deep-sea drilling project
FPC	Fugro pressure corer
FRPC	the Fugro Rotary Pressure Core
HRC	HYACE Rotary Corer
HYACE	Hydrate coring equipment system
Hybrid-PCS	the Hybrid-Pressure Core Sampler
IPP-Coring	*In-situ* pressure-preserved coring
IPTC	Instrumented Pressure Testing Chamber
JIP	the Joint Industry Project
JOGMEC	Japan Oil, Gas and Metals National Corporation
MAC	Multiple autoclave corer
NGH	Natural gas hydrate
ODP	Ocean Drilling Program
PCB	Pressure core barrel
PCS	Pressure core sampler
PCTB	Pressure Core Tool with Ballvalve
PTCS	Pressure temperature core sampler
PTPS	Pressure and temperature preservation system
SUCO	the Submarine Gas Hydraulic Reserves corer

List of symbols

h	the positive scalar function
L	the loading criterion function
$\{d\sigma\}$	the stress increment, MPa
$\{d\varepsilon^e\}$	the elastic strain increment
$[C]$	the tensor of elastic modulus in matrix form
$\{d\varepsilon\}$	the total strain increment
$\{d\varepsilon^p\}$	the plastic strain increment
$d\lambda$	the scalar function
$\{\partial g/\partial\{\sigma\}\}$	the gradient vector of the plastic potential function
ω	the stress deviation rate
σ_N	the stress values without rotation, MPa
σ_R	the stress values after a certain angle of rotation, MPa

- the assessment of natural hazards brought about by large-scale mining and the formulation of corresponding preventive measures (Borowski et al., 1996; Chen and Guo, 1998; Collett, 2002; Wang and Sun, 2009; Gao et al. 2018, 2020; Veluswamy and Linga, 2021).

However, the formation mechanism of NGH reservoirs is very complex (Zhang et al., 2011; Shagapov and Tazetdinov 2014). During sampling, core recovery or subsequent testing, if the temperature and pressure environment of NGH changes, then the physical properties, internal structure and mechanical properties of hydrate-bearing sediments may change to a statistically significant extent (Gao et al. 2020, 2021; He et al., 2021). It is difficult to retrieve *in situ* NGH. To solve this problem, *in-situ* pressure-preserved coring (IPP-Coring) has been developed as an effective method to extract hydrate deposits from underground sediments and preserve the samples under *in situ* hydrostatic pressure (Dai and Santamarina, 2014).

There are various pressure coring systems, but all of these systems aim to transfer unchanged cores to the surface (Li et al., 2016). In the 1970s, the early Pressure Core Barrel (PCB) was adopted by the Deep Sea Drilling Project (DSDP). The success rate of core recovery was very low due to the ball valve closing problem. In 1983, the international Ocean Drilling Program (ODP) developed the Pressure Core Sampler (PCS) and obtained samples of NGH without affecting their pressure from the Blake Outer Ridge. The sediment was recovered by a rotary or push rod coring machine and sealed by a ball valve. The operating pressure was 70 MPa. The first systematic pressure core sampling occurred during ODP 164 drilling in 1995. The Hydrate Autoclave Coring Equipment System (HYACE), funded by the European Union's Marine Science and Technology Program, was developed in the late 1990s. Two types of wireline pressure corers were developed within the HYACE: the Fugro Pressure Core (FPC) and the HYACE Rotary Corer (HRC) samplers. The more recent HYACINTH (Deployment of HYACE tools In New Tests on Hydrates) project is designed to transfer the collected cores from the coring device to the measuring chamber without pressure leakage. The HYACINTH system includes not only coring tools, such as the FPC, HRC, the Fugro Rotary Pressure Core (FRPC) and the Submarine Gas Hydraulic Reserves (SUGAR) corer (SUCO) but so a series of subsequent core testing and processing equipment. The MAC (Multiple Autoclave Corer) and DAPC (Dynamic Autoclave Piston Corer) were developed and used in Germany in 2002 and 2003, respectively. In 2005, the Joint Industry Project (JIP) used HYACE FPC and HRC to obtain pressure cores, and the Instrumented Pressure Testing Chamber (IPTC) instrument developed by USGS and Georgia Institute of Technology to analyze cores under *in situ* pressure environments. PCB, PCS, HRC and FPC could not maintain the *in situ* temperature. Therefore, Japan Oil, Gas and Metals National Corporation (JOGMEC) invented the PTCS (Pressure Temperature Core Sampler) for the first time, which can work under a pressure of 30 MPa and has been used in the Nankai Trough. The PTCS is effective in sandstone sediments. Since 2000, the Hybrid-Pressure Core Sampler (Hybrid-PCS) or Pressure Core Tool with Ballvalve (PCTB) has been used in offshore drilling projects in China (Zhang et al., 2019), the UK and other countries. The HYACE/Fugro FPC and FRPC systems are also used offshore Korea and in the Gulf of Mexico. In China, Zhejiang University developed a gravity piston-type coring device. Zhu et al. developed an NGH coring device with the Pressure and Temperature Preservation System (PTPS). A brief overview of the IPP-Coring is shown in Fig. 1.

In conclusion, core is the first complete data in the process of petroleum exploration and development. The pressure controller of the coring device is the key to the success of the IPP-Coring (Xie et al., 2021). Ball valve or flap valve is commonly used as the sealing structure in existing pressure coring devices. Among the hydrate-bearing sediment samples retrieved by pressure coring devices, more than 30% of the samples do not retain the pressure or only retain part of the *in situ* pressure, resulting in high deployments cost. This study proposes a new shell pressure controller with a novel spheric-cylindric structure intended to have a higher ultimate bearing strength and investigates its rotation failure. Further, the recovery rate of pressure maintaining coring is improved through failure mechanism analysis.

2. Design of spherical-cylindrical shell pressure controllers

The pressure controller is a sealing mechanism (generally a ball valve or flap valve) and determines the ultimate pressure strength of the pressure coring device (Gao et al., 2021). This paper presents a new principle of pressure coring for maintaining the coring pressure. The valve cover of the pressure controller is initially erected in the corer (shown in Fig. 2). When the coring is completed, the inner cylinder is released. Then, the valve cover

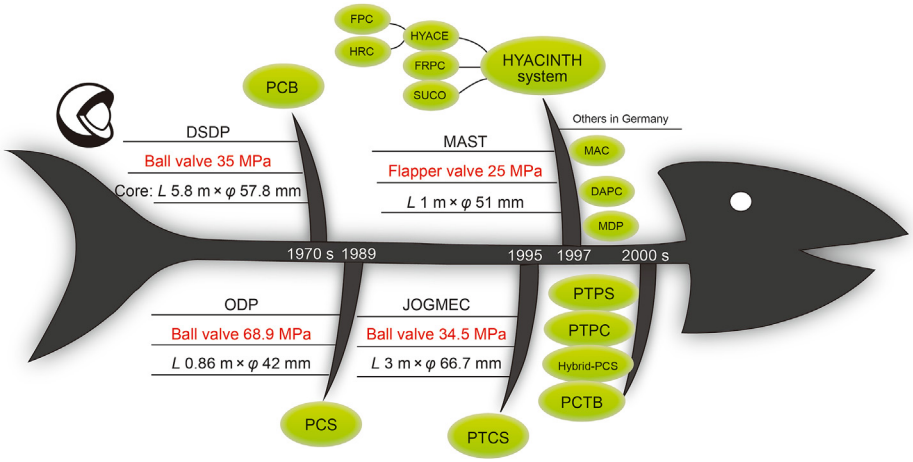

Fig. 1. A brief overview of pressure coring technologies.

turns over to the matching valve seat. Flapper valve sealing mechanisms can maximize the core diameter and downhole drive mechanisms to ensure core quality. Based on the principle of intersecting spherical shells and cylindrical shells, this new configuration, referred to as a spherical-cylindrical shell pressure controller (Fig. 2), is proposed. The spherical-cylindrical shell pressure controller consists of a cylindrical valve cover with a spherical edge and a matching seat. The traditional conical contact has a horizontal thrust, which greatly affects the pressure-preserved capacity of the IPP-Coring. The new structure adjusts the contact form between the valve cover and the valve seat so that there is only a normal support force. Compared with the conventional conical pressure controller, the spherical-cylindrical shell pressure controller has smaller structural deformation and higher bearing strength (Li et al., 2021). However, the contact pattern of the spherical-cylindrical shell pressure controller is similar to that of the spherical hinge. Thus, the two parts easily rotate around the common spherical center (Fig. 3). The maintenance of oil and gas pressure puts forward strict requirements for the performance of the structure (Li et al., 2021). The rotation failure of the pressure controller needs to be further studied.

3. Influence of rotation angle on spherical-cylindrical shell pressure controllers

3.1. Simulation procedures

ABAQUS is a powerful engineering numerical simulation software based on finite element method, which can solve linear and nonlinear problems in a wide range of fields. In the paper, to analyze the failure mechanism of the structure, numerical simulation is carried out based on ABAQUS software. The elastoplastic model is adopted, which is based on the fundament assumptions of isotropic elasticity continuum, i.e., elasticity, homogeneity, isotropy and small deformation (see Fig. 4).

Based on the ABAQUS/CAE User's Manual and elasto-plasticity theory (Lubarda, 2002), the general constitutive equation for an elastic-plastic material is briefly introduced. The stress increment, $\{d\sigma\}$ can be expressed in terms of the elastic strain increment, $\{d\varepsilon^e\}$, as

$$\{d\sigma\} = [C]\{d\varepsilon^e\} = [C](\{d\varepsilon\} - \{d\varepsilon^p\}) \quad (1)$$

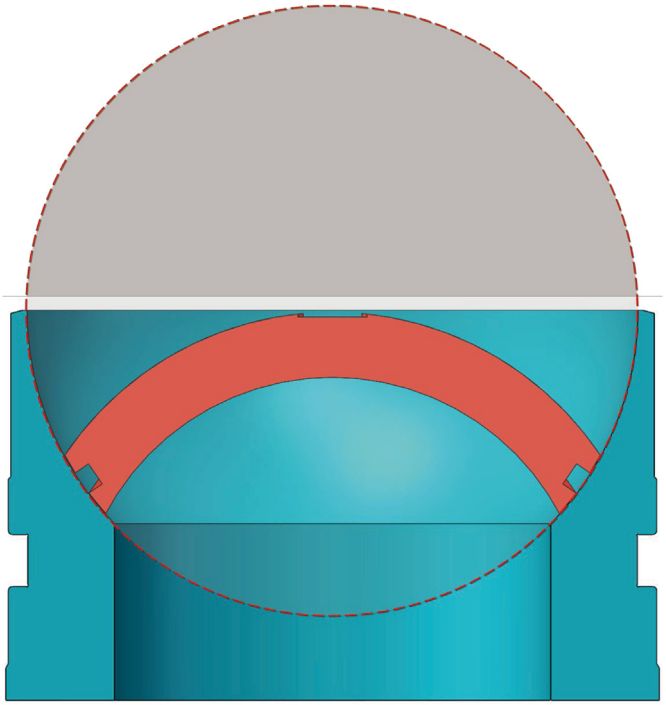

Fig. 2. Spherical-cylindrical shell pressure controller.

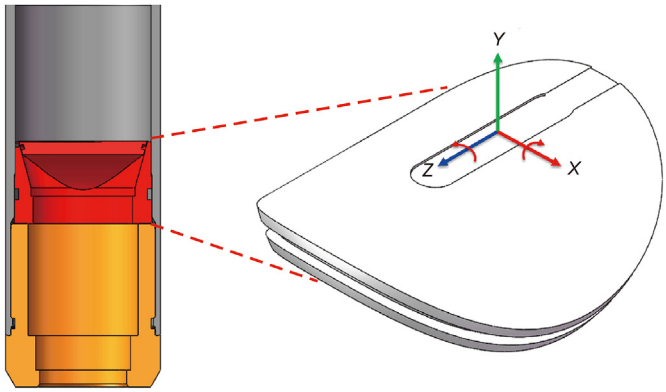

Fig. 3. Rotation of spherical-cylindrical shell pressure controllers.

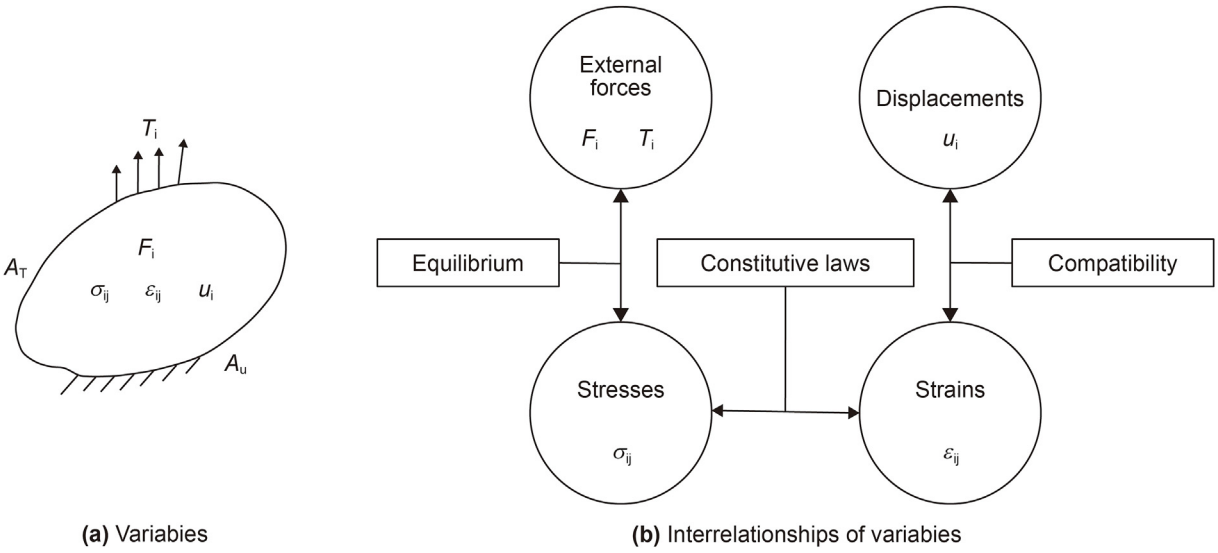

Fig. 4. Establishment of a solid mechanics problem.

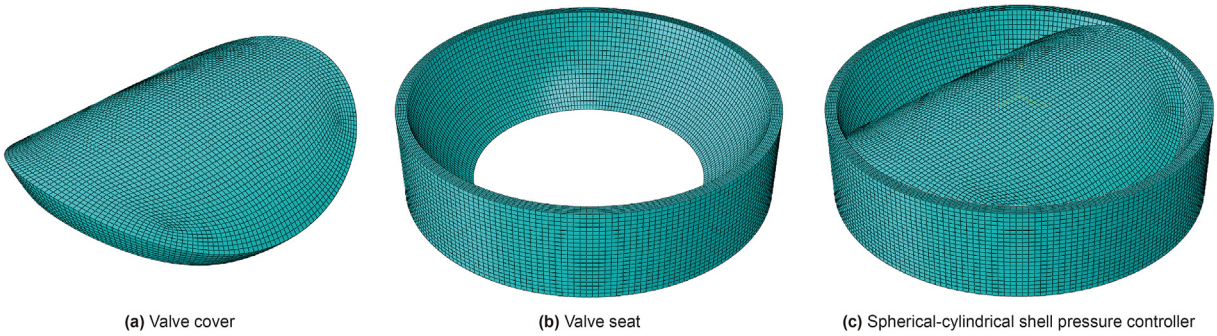

Fig. 5. The mesh of a spherical-cylindrical shell pressure controller.

and

$$\{d\varepsilon^p\} = d\lambda\left\{\frac{\partial g}{\partial\{\sigma\}}\right\} = \frac{L}{h}\left\{\frac{\partial g}{\partial\{\sigma\}}\right\} \tag{2}$$

with

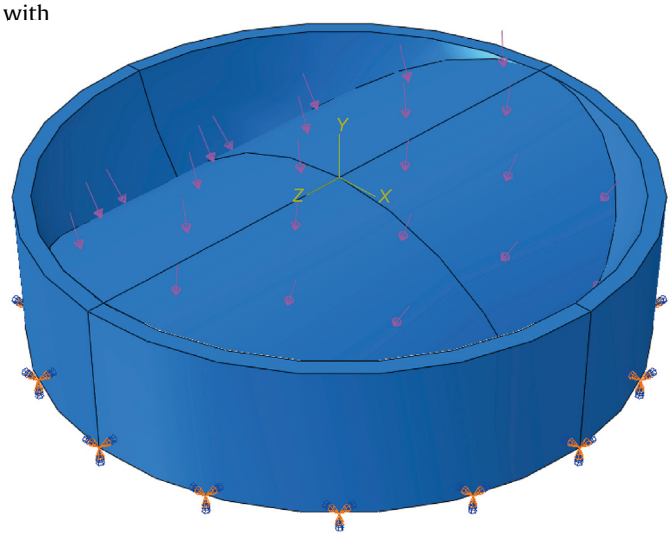

Fig. 6. Boundary conditions.

$$L = \left\{\frac{\partial f}{\partial\{\sigma\}}\right\}^T [C]\{d\varepsilon\} \tag{3}$$

where $[C]$ is the tensor of elastic modulus in matrix form, $\{d\varepsilon\}$ is the total strain increment, $\{d\varepsilon^p\}$ is the plastic strain increment, $d\lambda$ is the scalar function, $\{\partial g/\partial\{\sigma\}\}$ is the gradient vector of the plastic potential function, L is the loading criterion function, h is the positive scalar function. The stress calculation will be performed for all Gaussian sampling points.

3.2. Model setup

To study the stress distribution and failure mechanism, a geometric model (shown in Fig. 5) is established. The sealing groove is simplified. Hexahedral mesh is used. The boundary condition is shown in Fig. 6. The underside of the seat is fully restrained. A simulated *in situ* hydrostatic pressure is applied to the top surface of the valve cover. Alloy 304 stainless steel is used as the test material. The original gauge length of the specimen is 32 mm. The tensile test (shown in Fig. 7) is carried out on a Shimadzu electronic testing machine. The yield strength and tensile strength are 613.6 MPa and 828.6 MPa, respectively. The friction coefficient of the contact surface is 0.2.

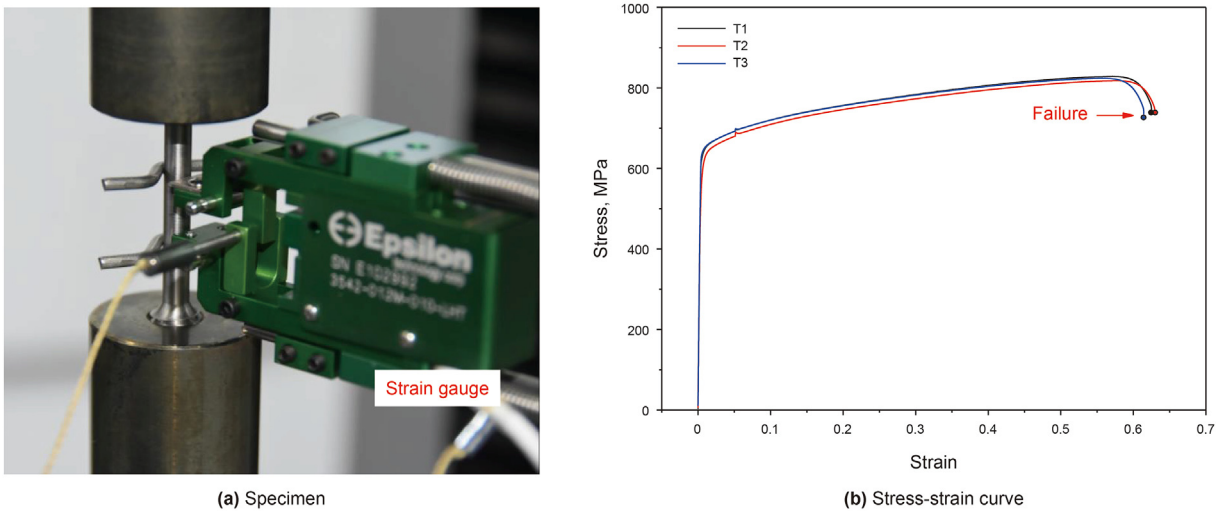

(a) Specimen **(b)** Stress-strain curve

Fig. 7. Tensile test results of stainless steel.

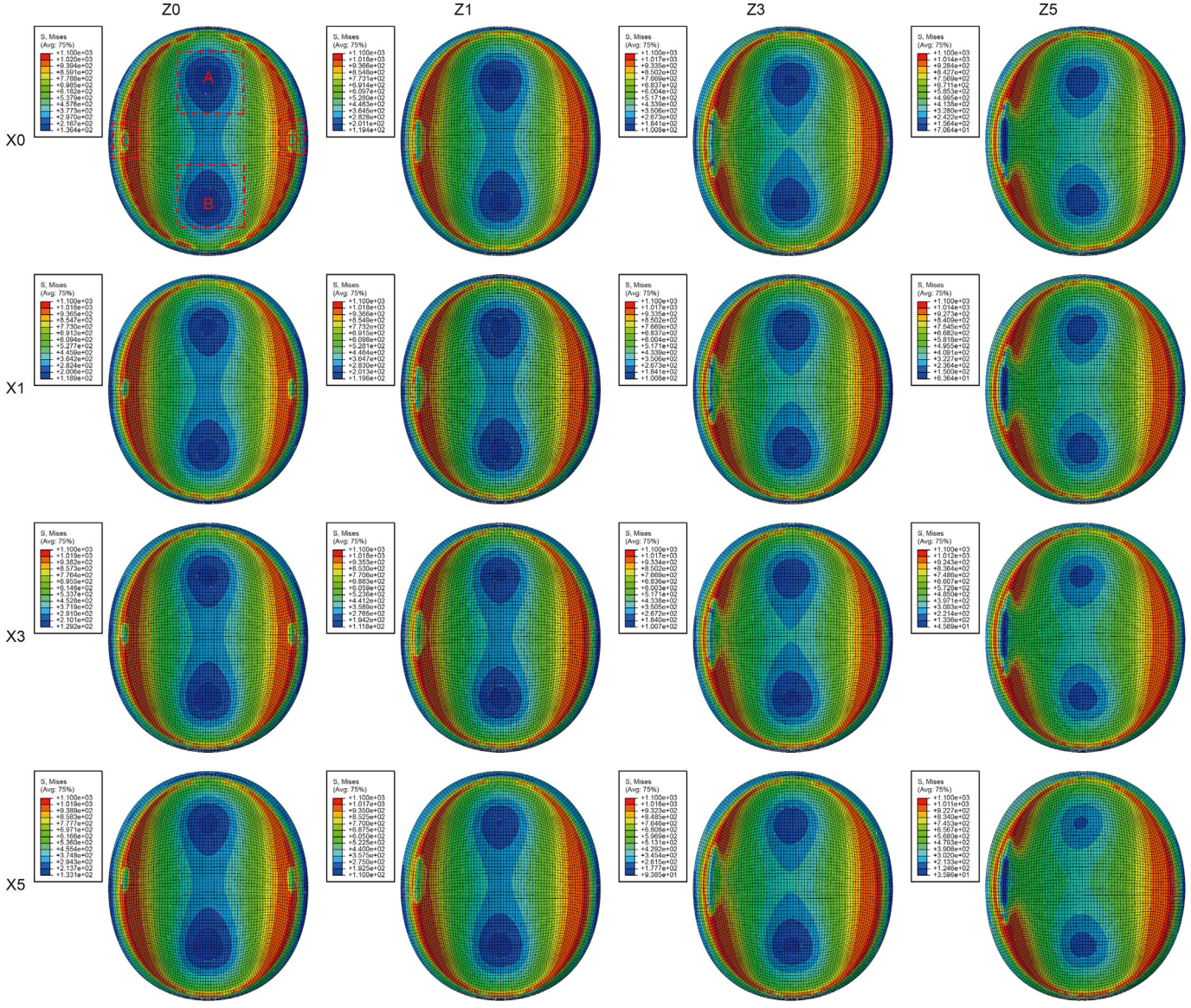

Fig. 8. Equivalent stress distribution of valve cover with different rotation angles.

3.3. Simulation results

The stress distribution of the valve cover is shown in Fig. 8 with different rotation angles. There are two low stress zones, A and B, in the middle bottom surface of the valve cover. With the increase in the z-axis rotation angle, the left equivalent stress gradually decreases, and the left low stress area C expands. With the increase in the rotation angle around the x-axis and z-axis, the equivalent stresses in A and D increase continuously. The equivalent stress in zone C decreases continuously. This means that zone C may not be able to provide effective sealing pressure, which is the potential weak site of leakage.

Three measuring lines are defined (as shown in Fig. 9 (a)) where L1 and L2 are the monitoring lines along the minor axis and major axis, respectively, and L3 is the circumferential monitoring line of the valve cover. Fig. 9 (b) shows that with increasing z-axis rotation angle, the stress on L1 shows a decreasing trend. The stress deviation rate is defined as

$$\omega = \frac{\sigma_R - \sigma_N}{\sigma_N} \times 100\% \tag{4}$$

where ω is the stress deviation rate, and σ_N and σ_R are the stress values without rotation and after a certain angle of rotation, respectively.

The stress deviation rates of L1 are −11.2, −75.4, and −92.6% when rotating 1, 3, and 5° around the z-axis and rotating 0° around the x-axis. Fig. 9 (c) and Fig. 9 (d) show the stress distributions of the L1 and L2 measuring lines with different x-axis rotation angles. With the increase in the x-axis rotation angle, the stress deviation increases gradually. Compared with the x-axis rotation, the rotation around the z-axis has a more obvious effect on the stress deviation of L1. In fact, spherical-cylindrical shell pressure controllers may simultaneously experience the influences of x-axis and z-axis rotations. Fig. 10 shows the stress distribution of L1 under the xz compound rotation. When rotating 5° around the x-axis, the stress deviation rates for 0, 1, 3 and 5° around the z-axis are −10.7, −58.9, −72.2 and −92.4%, respectively. The larger the x-axis rotation angle is, the greater the stress drop.

According to the numerical simulation results, the valve cover can form a strong support along the major axis. The low stress zone C is likely to be the weak site of leakage. The deformation along the minor axis is the main factor affecting the structural strength of the valve cover. The effect of z-axis rotation on the monitoring line L3 is much higher than that of the x-axis (see Fig. 11). For instance, when rotating 5° around the z-axis and 0° around the x-axis, the stress deviation rate reaches 92.6%. It is difficult to provide enough contact pressure for the sealing surface. Finally, the overall strength of the pressure controller is invalid. In the engineering practice of pressure coring, the sealing performance is very important for

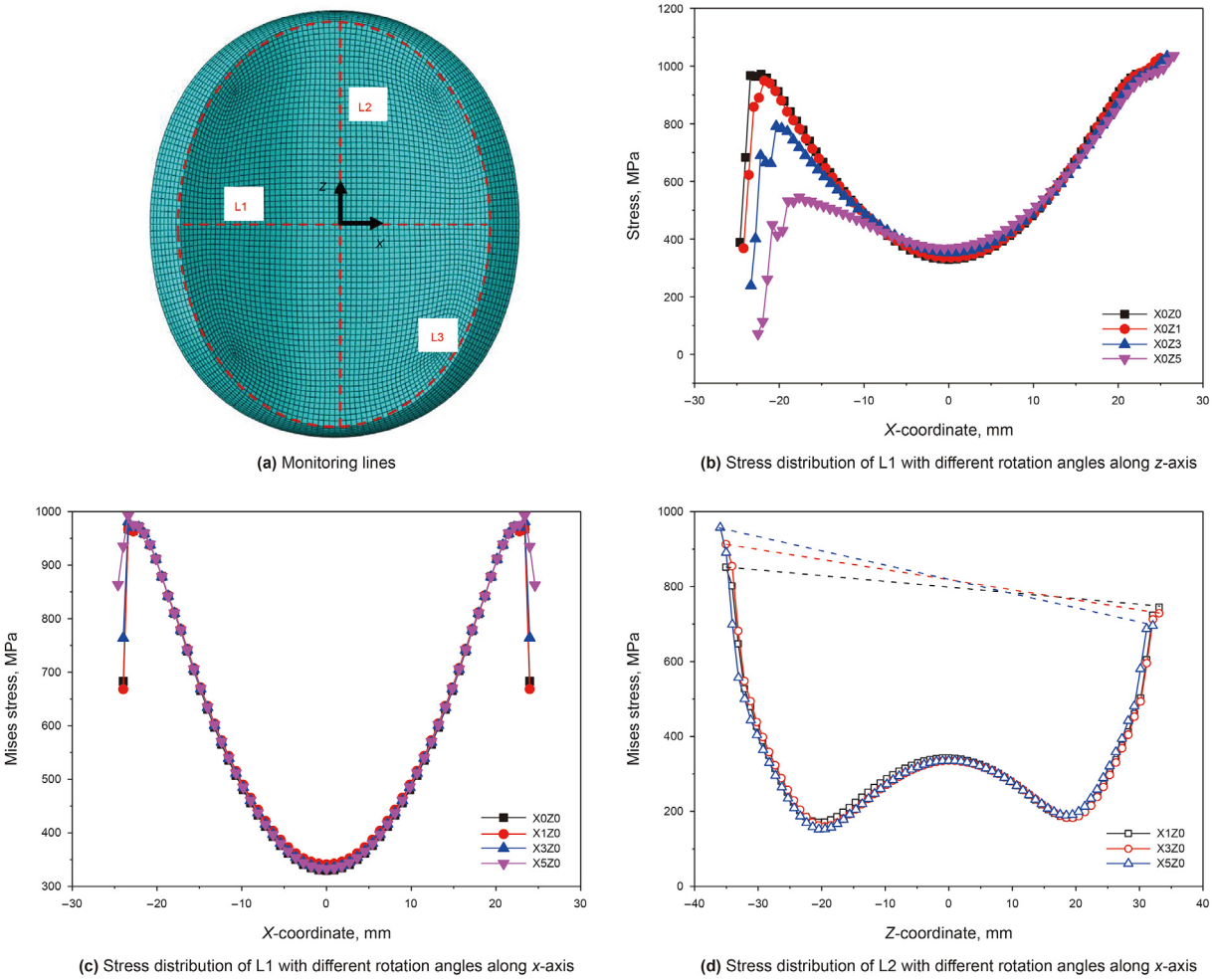

(a) Monitoring lines

(b) Stress distribution of L1 with different rotation angles along *z*-axis

(c) Stress distribution of L1 with different rotation angles along *x*-axis

(d) Stress distribution of L2 with different rotation angles along *x*-axis

Fig. 9. Equivalent stress distribution of different measuring lines.

maintaining oil and gas pressure. Due to the stress redistribution during the rotation of the structure, the stress at the edge of the valve cover is reduced, and the fluid medium with pressure will leak from the contact surfaces.

4. Failure pressure of spherical shell pressure controller

The deformation characteristics and sealing stability of the pressure controller are very important to the success rate of pressure coring. However, there is no special test device for evaluating pressure controllers domestically and abroad. Therefore, we developed a pressure controller test platform that, according to the size of the coring device, can test the failure pressure of pressure controllers with different configurations.

4.1. Testing system

To obtain the failure pressure of the spherical-cylindrical shell pressure controllers under different working conditions, an experimental platform (Fig. 12) was designed in this laboratory. The specimen was installed inside the test chamber. Then, water was pumped to the chamber through the injection port until the specimen failed. The watertight joint provided a data channel for the strain gauge at the top of the valve cover. According to the numerical simulations, the positions of three strain gauges were determined. Among them, SG-1, SG-2 and SG-3 were the equivalent stress concentration area, the large deformation area and the stress concentration edge, respectively.

4.2. Physical experiment results

Two tests were carried out based on the test system. The pressure controllers before and after the test are shown in Fig. 13(a). Under the condition of high pressure, the sealing ring was damaged due to the insufficient contact pressure in the weak area C.

Fig. 14(a) shows that with the increasing load, the strains of SG-1Z and SG-2Z were gradually increasing tensile deformation, while the strains of SG-1X, SG-2X and SG-3X were compressive deformation. After a certain rotation angle, the ultimate bearing strength was only 8.4 MPa. After the failure of the pressure controller, the pressure in the test chamber decreases, and the strain data tended to zero. The compressive strains in SG-1X and SG-2X were the largest, 4.02×10^{-4} and 4.43×10^{-4}, respectively. Torsional instability occurred in the pressure controller, and the force on the valve cover was uneven. There was a notch on one side of the seat (Fig. 15). According to the second test results under the same conditions, the maximum bearing strength of the spherical pressure controller was 43.8 MPa (shown in Fig. 14(b)). There was a great gap due to the rotation of the structure. Therefore, it was necessary to add a limiting surface to reduce the rotation of the structure.

According to the numerical simulations and laboratory tests, the bearing strengths are greatly reduced by rotation to any angle. The strains predicted by the numerical simulations are basically consistent with the experimental results. As seen from Fig. 16, the strain on the left side of the cover is very small, which means that the contact pressure at this position is small. The sealing ring is

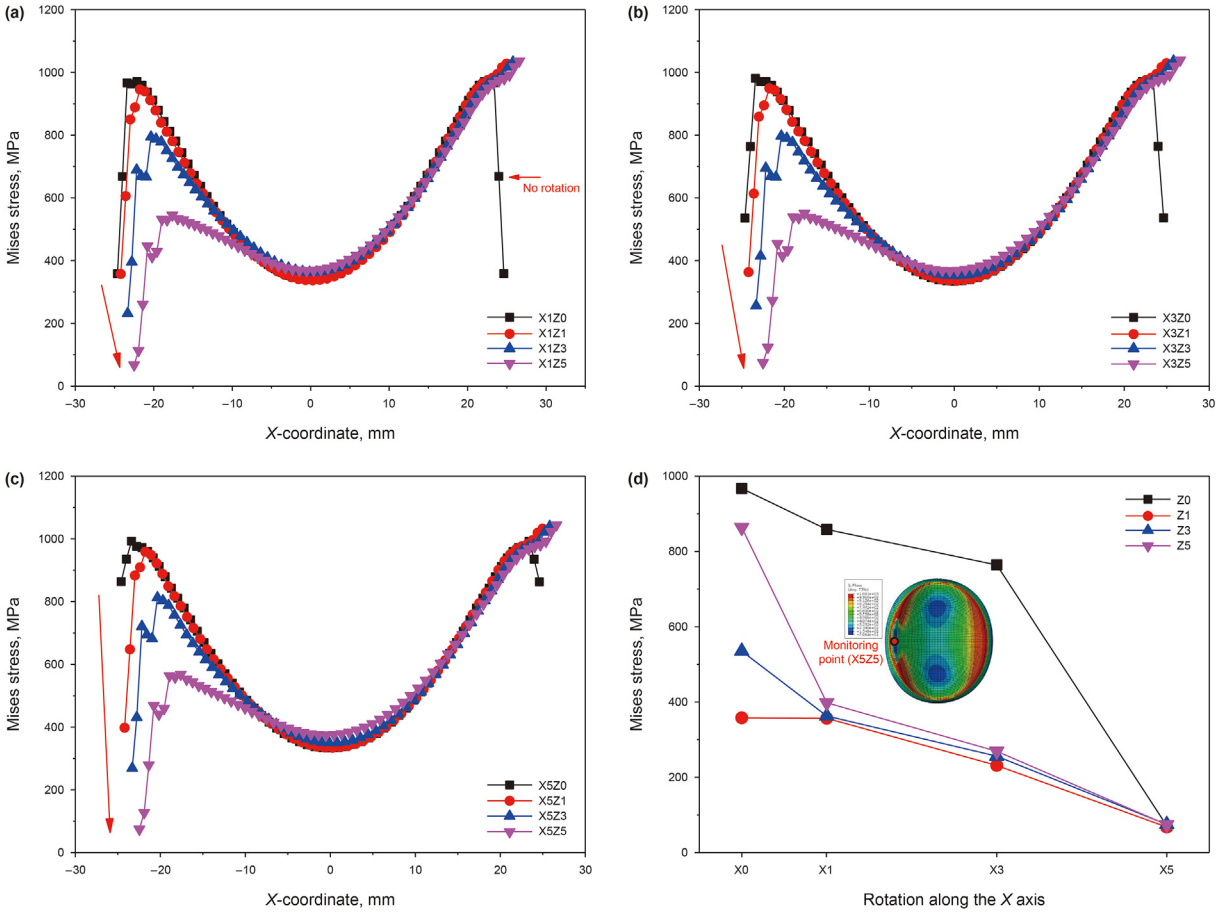

Fig. 10. Stress distribution of L1 under XZ compound rotation.

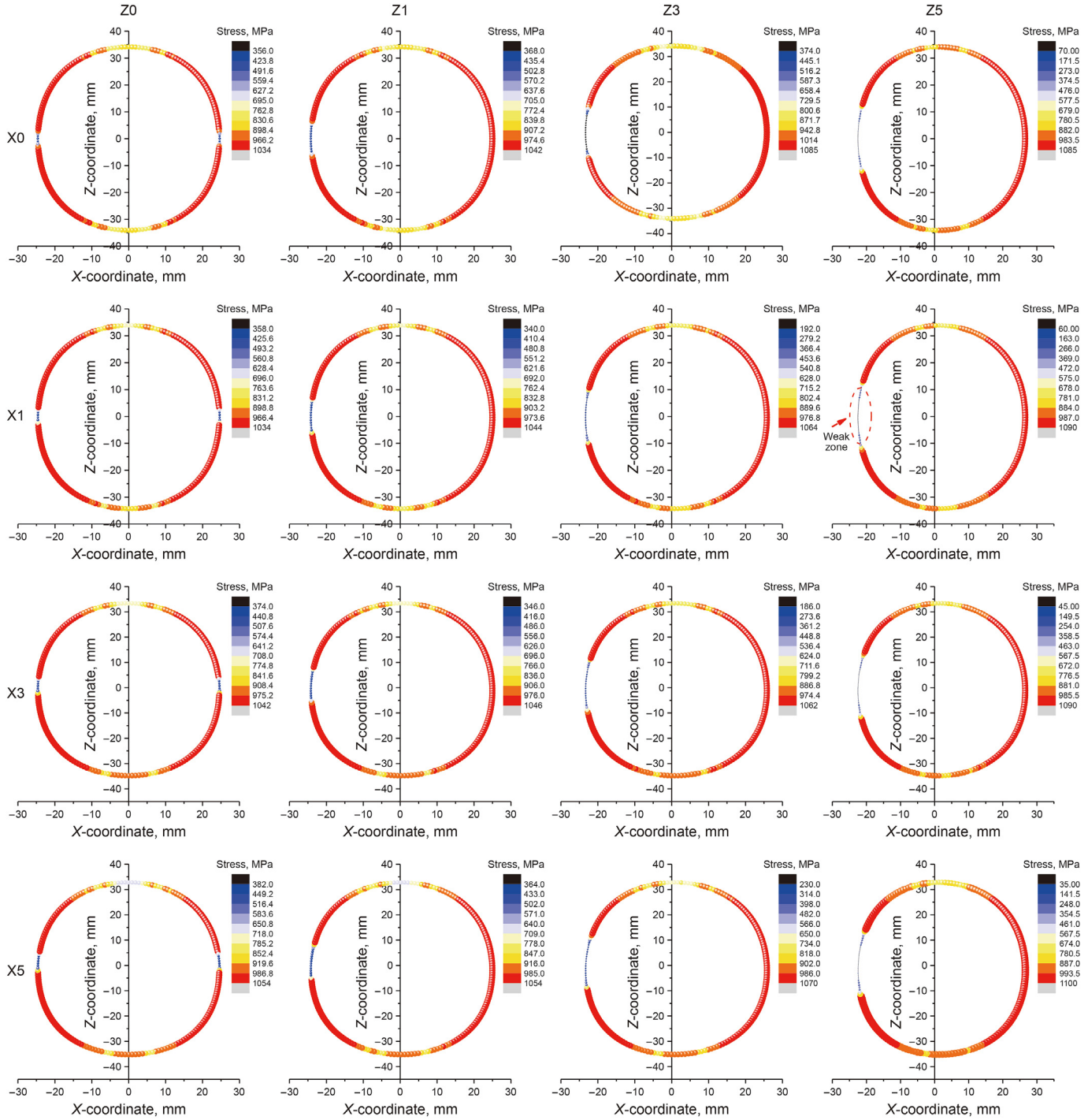

Fig. 11. Equivalent stress distributions of L3 under different rotation angles.

extruded from the enlarged gap, which is consistent with the physical experimental results. Therefore, by adjusting the angle of the valve cover, the structural strength is increased from 8.4 to 43.8 MPa.

The *in situ* physical and mechanical properties are crucial for deep oil and gas exploration. The paper focuses on the pressure controllers, which is one of the key components of deep-sea pressure coring device. It can obtain cores with deep-sea *in situ* pressure. On the one hand, pressure cores are the premise of quantitative evaluation of *in situ* permeability and saturation of oil and gas. It is of great significance for understanding geological conditions, evaluating recoverable reserves and improving recovery rate. On the other hand, it provides a technical means for the study of *in situ* mechanical parameters of natural gas hydrate, affecting the efficiency of industrial production. Through the research of this paper, the strength of the developed IPP-Coring can be suitable for *in situ* applications at depths of thousands of meters, and cores with higher pressures can be obtained. This capability of

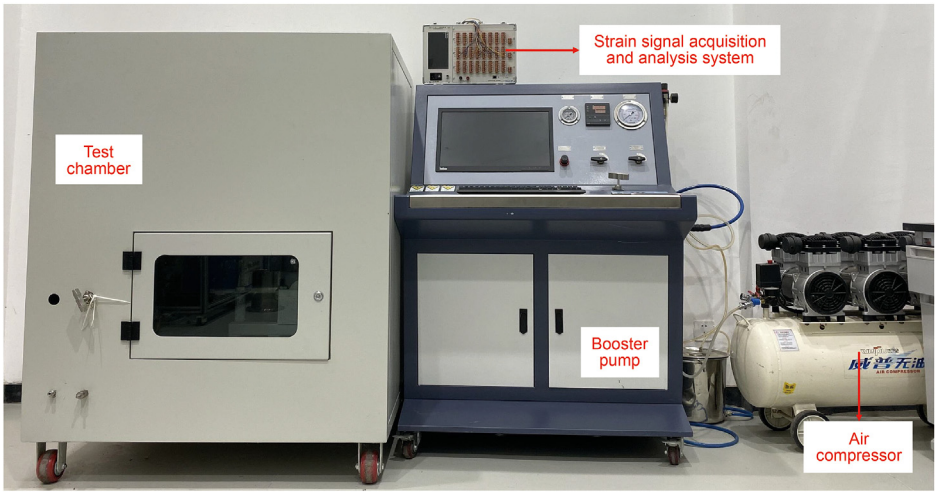

Fig. 12. Test equipment designed in this laboratory.

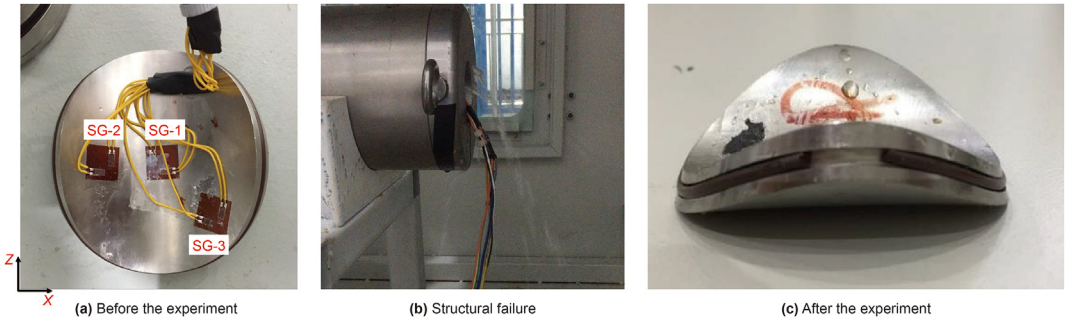

Fig. 13. Spherical pressure controller.

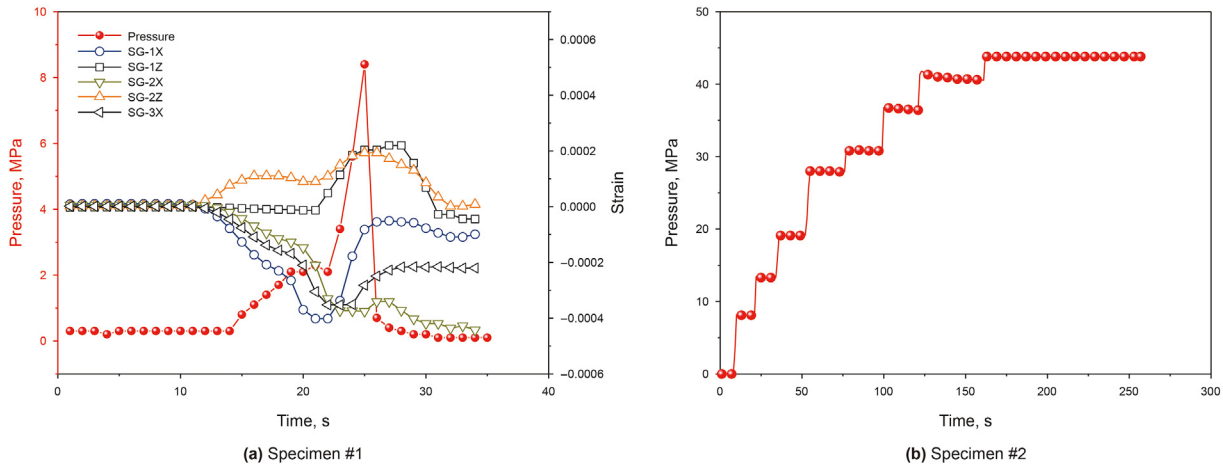

Fig. 14. Physical test results.

the newly developed pressure coring device not only effectively ensures the safety and lives of on-site operators, but also brings certain economic benefits.

5. Conclusion

The conclusions are as follows:

1. Based on the principle of intersecting spherical shells and cylindrical shells, a new structure for a spherical-cylindrical shell pressure retaining controller is designed. Through numerical simulation and experimental test, its ultimate bearing strength reaches 43.8 MPa.
2. The rotation of the valve cover increases the deformation of the valve cover, which greatly reduces the contact pressure of the sealing surface, resulting in sealing failure. To quantitatively

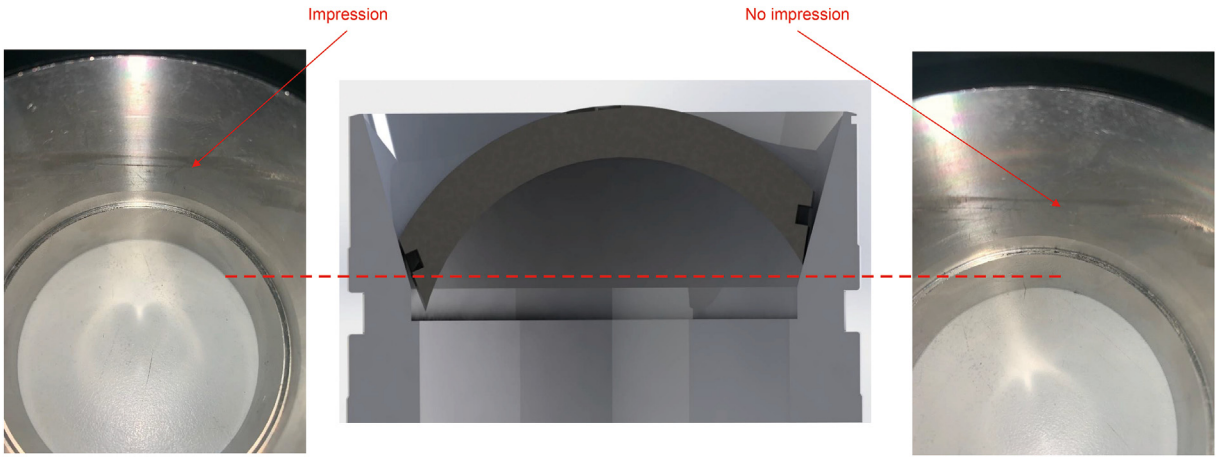

Fig. 15. Unbalanced notch in the valve seat caused by structural rotation.

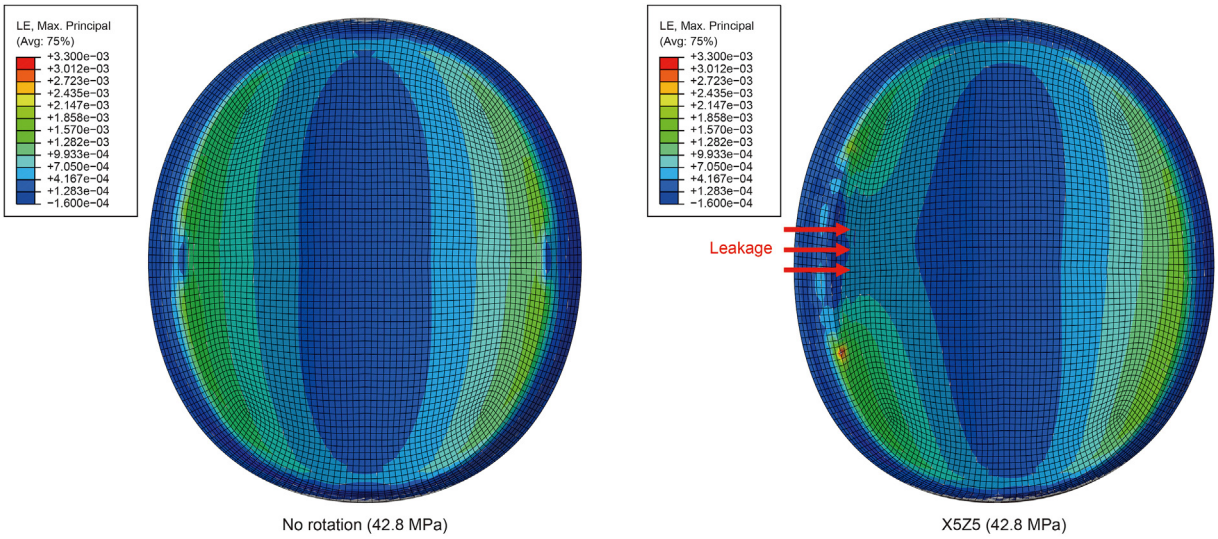

Fig. 16. Strain of the pressure controller.

characterize the stress concentration caused by the rotation, the stress deviation rate is defined. The effect of z-axis rotation is much greater than that of x-axis rotation. When rotating 5° around the z-axis, the equivalent stress drop is - 92.6%.

3. The contact pressure reduction caused by rotation is the root cause of the failure of the pressure maintaining controller. To prevent the rotational failure, an anti-rotation structure should be adopted to control the valve cover rotation within 1° around the major axis.

IPP-Coring has a great influence on the measurement of oil and gas saturation parameters. The fluid saturation provided by analysis of core obtained by pressure coring can better represent the original reservoir state than that provided by conventional core analysis, especially in cases of the evaluation of gas reservoir reserves and the feasibility of enhanced oil recovery. This study reveals the rotation failure principle of spherical pressure controllers, which can help to improve the success rate of pressure coring and provide technical support for the exploration and evaluation of deep oil and gas resources.

Declaration of competing interest

The authors declare that they have no known competing financial interests or personal relationships that could have appeared to influence the work reported in this paper.

Acknowledgments

The paper was supported by the Program for Guangdong Introducing Innovative and Enterpreneurial Teams (No. 2019ZT08G315) and National Natural Science Foundation of China No. 51827901 and U2013603.

References

Archer, D.F., 2007. Methane hydrate stability and anthropogenic climate change. Biogeosciences 4 (4). https://doi.org/10.5194/bgd-4-993-2007.

Aydin, H., Merey, S., 2021. The effect of gas production from deeper conventional gas reservoirs on shallower gas hydrate layer stability: a case study in the conditions of the Sakarya gas field, Western Black Sea. J. Nat. Gas Sci. Eng. 94, 104103. https://doi.org/10.1016/j.jngse.2021.104103.

Borowski, W.S., Paull, C.K., Ussler, W., 1996. Marine pore-water sulfate profiles indicate in situ methane flux from underlying gas hydrate. Geology 24 (7), 655–658.

Boswell, R., Collett, T., 2011. Current perspectives on gas hydrate resources. Energy Environ. Sci. 4, 1206–1212. https://doi.org/10.1039/c0ee00203h.
Chen, G.J., Guo, T.M., 1998. A new approach to gas hydrate modelling. Chem. Eng. J. 71 (2), 145–151. https://doi.org/10.1016/S1385-8947(98)00126-0.
Collett, T.S., 2002. Energy resource potential of natural gas hydrates. AAPG Bull. 86 (11), 1971–1992. https://doi.org/10.1016/S0031-0182(02)00486-8.
Dai, S., Santamarina, J.C., 2014. Sampling disturbance in hydrate-bearing sediment pressure cores: NGHP-01 expedition, Krishna-Godavari Basin example. Mar. Petrol. Geol. 58, 178–186. https://doi.org/10.1016/j.marpetgeo.2014.07.013.
Dickens, G.R., Paull, C.K., Wallace, P., 1997. Direct measurement of *in situ* methane quantities in a large gas-hydrate reservoir. Nature 385 (6615), 426–428. https://doi.org/10.1038/385426a0.
Fu, C., Guo, B., Lee, J., 2021. Mathematical modeling of heat transfer in y-shaped well couples for developing gas hydrate reservoirs using geothermal energy. J. Nat. Gas Sci. Eng. 104325. https://doi.org/10.1016/j.jngse.2021.104325.
Gao, M., Xie, J., Gao, Y., et al., 2021. Mechanical behavior of coal under different mining rates: a case study from laboratory experiments to field testing. Int. J. Min. Sci. Technol. 31, 825–841. https://doi.org/10.1016/j.ijmst.2021.06.007.
Gao, M., Xie, J., Guo, J., et al., 2021. Fractal evolution and connectivity characteristics of mining-induced crack networks in coal masses at different depths. Geomech. Geophys. Geo-Energy Geo-Resour. 7 (1). https://doi.org/10.1007/s40948-020-00207-4.
Gao, M.Z., Chen, L., Fan, D., et al., 2021. Principle and technology of coring with in-situ Pressure and gas maintaining in deep coal mine. J. China Coal Soc. 46 (3), 885–8997 (**in Chinese**).
Gao, M.Z., Hao, H.C., Xue, S.N., et al., 2021. Discing behavior and mechanism of cores extracted from Songke-2 well at depths below 4,500 m. Int. J. Rock Mech. Min. Sci. 149. https://doi.org/10.1016/j.ijrmms.2021.104976.
Gao, M.Z., Liu, J.J., Lin, W.M., et al., 2020a. Study on in-situ stress evolution law of ultra-thick coal seam in advance mining. Coal Sci. Technol. 48 (2), 8 (**in Chinese**).
Gao, M.Z., Wang, M.Y., Xie, J., et al., 2021. Experimental study on the mechanical response mechanism of different unloading rate to coal rock mechanics. Adv. Eng. Sci. 53 (6), 54–63 (**in Chinese**).
Gao, M.Z., Yang, B.G., Xie, J., et al., 2022. The mechanism of microwave rock breaking and its potential application to rock-breaking technology in drilling. Petrol. Sci. https://doi.org/10.1016/j.petsci.2021.12.031.
Gao, M.Z., Zhang, J.G., Li, S.W., et al., 2020b. Calculating changes in fractal dimension of surface cracks to quantify how the dynamic loading rate affects rock failure in deep mining. J. Cent. S. Univ. 27 (10), 3013–3024. https://doi.org/10.1007/s11771-020-4525-5.
Gao, M.Z., Zhang, Z.L., Yin, X.G., et al., 2018. The location optimum and permeability-enhancing effect of a low-level shield rock roadway. Rock Mech. Rock Eng. 51, 2935–2948. https://doi.org/10.1007/s00603-018-1461-x.
He, Z.Q., Xie, H.P., Gao, M.Z., et al., 2021a. Research on properties of hollow glass microspheres/epoxy resin composites applied in deep rock in-situ temperature-preserved coring. Petrol. Sci. 21. https://doi.org/10.1016/j.petsci.2021.10.028.
He, Z.Q., Xie, H.P., Gao, M.Z., et al., 2021b. The fracturing models of hard roofs and spatiotemporal law of mining-induced stress in a top coal caving face with an extra-thick coal seam. Geomech. Geophys. Geo-Energy Geo-Resour. 7 (1). https://doi.org/10.1007/s40948-020-00202-9.
Hu, Y.Q., Xie, J., Xue, S.N., et al., 2021. Research and application of thermal insulation effect of natural gas hydrate freezing corer based on the wireline-coring principle. Petrol. Sci. https://doi.org/10.1016/j.petsci.2021.11.019.
Huang, W., Feng, G., He, H.L., et al., 2021. Development of an ultra-high-pressure rotary combined dynamic seal and experimental study on its sealing performance in deep energy mining conditions. Petrol. Sci. https://doi.org/10.1016/j.petsci.2021.11.020.
Jin, Y., Konno, Y., Nagao, J., 2014. Pressurized subsampling system for pressured gas-hydrate-bearing sediment: microscale imaging using X-ray computed tomography. Rev. Sci. Instrum. 85 (9), 367-328.
Jing, C.F., Yi, W., Xiao, S.L., et al., 2015. Production behaviors and heat transfer characteristics of methane hydrate dissociation by depressurization in conjunction with warm water stimulation with dual horizontal wells. Energy 79, 315e324. https://doi.org/10.1016/j.energy.2014.11.018.
Kida, M., Yoneda, J., Masui, A., et al., 2021. Mechanical properties of polycrystalline tetrahydrofuran hydrates as analogs for massive natural gas hydrates. J. Nat. Gas Sci. Eng. 96, 104284. https://doi.org/10.1016/j.jngse.2021.104284.
Konno, Y., Jin, Y., Uchiumi, T., et al., 2013. Multiple-pressure-tapped core holder combined with X-ray computed tomography scanning for gasewater permeability measurements of methane-hydrate-bearing sediments. Rev. Sci. Instrum. 84 (6), 064501. https://doi.org/10.1063/1.4811379.
Li, C., Xie, H.P., Gao, M.Z., et al., 2021b. Novel designs of pressure controllers to enhance the upper pressure limit for gas-hydrate-bearing sediment sampling. Energy (5), 120405. https://doi.org/10.1016/j.energy.2021.120405.
Li, J.N., Wang, J., Hu, Y.Q., et al., 2021a. Contact performance analysis of pressure controller's sealing interface in deep in-situ pressure-preserved coring system. Petrol. Sci. https://doi.org/10.1016/j.petsci.2021.11.022.
Li, L., Peng, J., Gao, Q., et al., 2016. Pressure retaining method based on phase change for coring of gas hydrate-bearing sediments in offshore drilling. Appl. Therm. Eng. 107, 633–641. https://doi.org/10.1016/j.applthermaleng.2016.06.174.
Lubarda, V.A., 2002. Elastoplasticity Theory.
Pang, X.Q., Chen, Z.H., Jia, C.Z., et al., 2021. Evaluation and re-understanding of the global natural gas hydrate resources. Petrol. Sci. 18, 323–338. https://doi.org/10.1007/s12182-021-00568-9.
Ruan, X., Li, X.-S., Xu, C.-G., 2021. A review of numerical research on gas production from natural gas hydrates in China. J. Nat. Gas Sci. Eng. 85, 103713. https://doi.org/10.1016/j.jngse.2020.103713.
Saberi, A., Alamdari, A., Rasoolzadeh, A., et al., 2021. Insights into kinetic inhibition effects of MEG,PVP,and L-tyrosine aqueous solutions on natural gas hydrate formation. Petrol. Sci. 18, 495–508.
Shagapov, V.S., Tazetdinov, B.I., 2014. Formation and dissociation of gas hydrate inclusions during migration in water. Thermophys. Aeromechanics 21 (3), 337–345. https://doi.org/10.1134/S086986431403007X.
Singh, S.C., Minshull, T.A., Spence, G.D., 1993. Velocity structure of a gas hydrate reflector. Science 260 (5105), 204–207. https://doi.org/10.1126/science.260.5105.204.
Sloan, E., 2003. Fundamental principles and applications of natural gas hydrates. Nature 426, 353–363. https://doi.org/10.1038/nature02135.
Veluswamy, H.P., Linga, P., 2021. Natural gas hydrate formation using saline/seawater for gas storage application. Energy Fuel. 35 (7). https://doi.org/10.1021/acs.energyfuels.1c00399.
Wang, Z., Sun, B., 2009. Annular multiphase flow behavior during deep water drilling and the effect of hydrate phase transition. Petrol. Sci. 6, 57–63. https://doi.org/10.1007/s12182-009-0010-3.
Xie, H.P., Liu, T., Gao, M.Z., et al., 2021. Research on in-situ condition preserved coring and testing systems. Petrol. Sci. https://doi.org/10.1016/j.petsci.2021.11.003.
Zhang, W., Liang, J., Wei, J., et al., 2019. Origin of natural gases and associated gas hydrates in the Shenhu area, northern South China sea: results from the China gas hydrate drilling expeditions. J. Asian Earth Sci. 183, 103953. https://doi.org/10.1016/j.jseaes.2019.103953.
Zhang, W., Ma, Q., Wang, R., et al., 2011. An experimental study of shear strength of gas-hydrate-bearing core samples. Petrol. Sci. 8, 177–182. https://doi.org/10.1007/s12182-011-0132-2.